# UC San Diego
## UC San Diego Previously Published Works

**Title**
Focal adhesions are foci for tyrosine-based signal transduction via GIV/Girdin and G proteins

**Permalink**
https://escholarship.org/uc/item/8096f4jx

**Journal**
Molecular Biology of the Cell, 26(24)

**ISSN**
1059-1524

**Authors**
Lopez-Sanchez, Inmaculada
Kalogriopoulos, Nicholas
Lo, I-Chung
et al.

**Publication Date**
2015-12-01

**DOI**
10.1091/mbc.e15-07-0496

Peer reviewed

# Focal adhesions are foci for tyrosine-based signal transduction via GIV/Girdin and G proteins

Inmaculada Lopez-Sanchez[a], Nicholas Kalogriopoulos[a], I-Chung Lo[b], Firooz Kabir[a], Krishna K. Midde[a], Honghui Wang[b], and Pradipta Ghosh[a,b]

[a]Department of Medicine and [b]Department of Cellular and Molecular Medicine, University of California, San Diego, School of Medicine, La Jolla, CA 92093

**ABSTRACT** GIV/Girdin is a multimodular signal transducer and a bona fide metastasis-related protein. As a guanidine exchange factor (GEF), GIV modulates signals initiated by growth factors (chemical signals) by activating the G protein Gαi. Here we report that mechanical signals triggered by the extracellular matrix (ECM) also converge on GIV-GEF via β1 integrins and that focal adhesions (FAs) serve as the major hubs for mechanochemical signaling via GIV. GIV interacts with focal adhesion kinase (FAK) and ligand-activated β1 integrins. Phosphorylation of GIV by FAK enhances PI3K-Akt signaling, the integrity of FAs, increases cell–ECM adhesion, and triggers ECM-induced cell motility. Activation of Gαi by GIV-GEF further potentiates FAK-GIV-PI3K-Akt signaling at the FAs. Spatially restricted signaling via tyrosine phosphorylated GIV at the FAs is enhanced during cancer metastasis. Thus GIV-GEF serves as a unifying platform for integration and amplification of adhesion (mechanical) and growth factor (chemical) signals during cancer progression.

## INTRODUCTION

The protein Gα-interacting, vesicle-associated (GIV; also known as Girdin) is a bona fide metastasis-related protein and a guanidine exchange factor (GEF) for trimeric Gi proteins that serves as a hub for enhancement of phosphoinositide 3-kinase (PI3K)-Akt signals (Garcia-Marcos et al., 2015). Ligand stimulation of a variety of receptors directly (e.g., growth factor receptor tyrosine kinases [RTKs]; Ghosh, 2015) or indirectly via non-RTKs (e.g., G protein–coupled receptors [GPCRs] and Toll-like receptors [TLRs]) triggers phosphorylation of GIV on two key tyrosines (Y1764 and Y1798) within its C-terminus, which directly bind and activate class 1 PI3Ks (Lin et al., 2011). GIV-dependent PI3K-Akt enhancement regulates a range of pathophysiologic processes in diverse cell types, including cancer

metastasis across a variety of solid tumors (Garcia-Marcos et al., 2015), epithelial wound healing (Ghosh et al., 2008), macrophage chemotaxis (Ghosh et al., 2008), myofibroblast activation during organ fibrosis (Lopez-Sanchez et al., 2014), podocyte survival after nephrotic injury (Wang et al., 2015), and insulin sensitivity in myoblasts (Hartung et al., 2013).

Mechanistically, GIV affects the aforementioned processes by modulating multi-RTK signaling at the plasma membrane (PM) via G protein intermediates, which in turn enhances tyrosine-based signaling through the RTK-GIV-PI3K axis (Ghosh, 2015; Lin et al., 2011, 2014). Despite these insights, the spatial configuration of such activated receptor–GIV signaling clusters remains unknown. Here we report that these activated signaling clusters predominantly localize to specialized concentrated patches at the PM called focal adhesions (FAs), which are mechanical sensors of environmental forces via integrins. Novel functional interactions with components of the FA enable GIV to serve as a common platform for both chemical sensing by RTKs and mechanosensing via integrins. Findings also illuminate how GIV's functions at the FAs may facilitate its widely recognized role in cancer metastasis.

## RESULTS AND DISCUSSION

### GIV localizes to FAs and is required for their integrity

We previously showed that GIV modulates growth factor RTK signaling via its ability to bind ligand-activated RTKs and couple them to activation of G proteins at the PM (Midde et al., 2015). To study
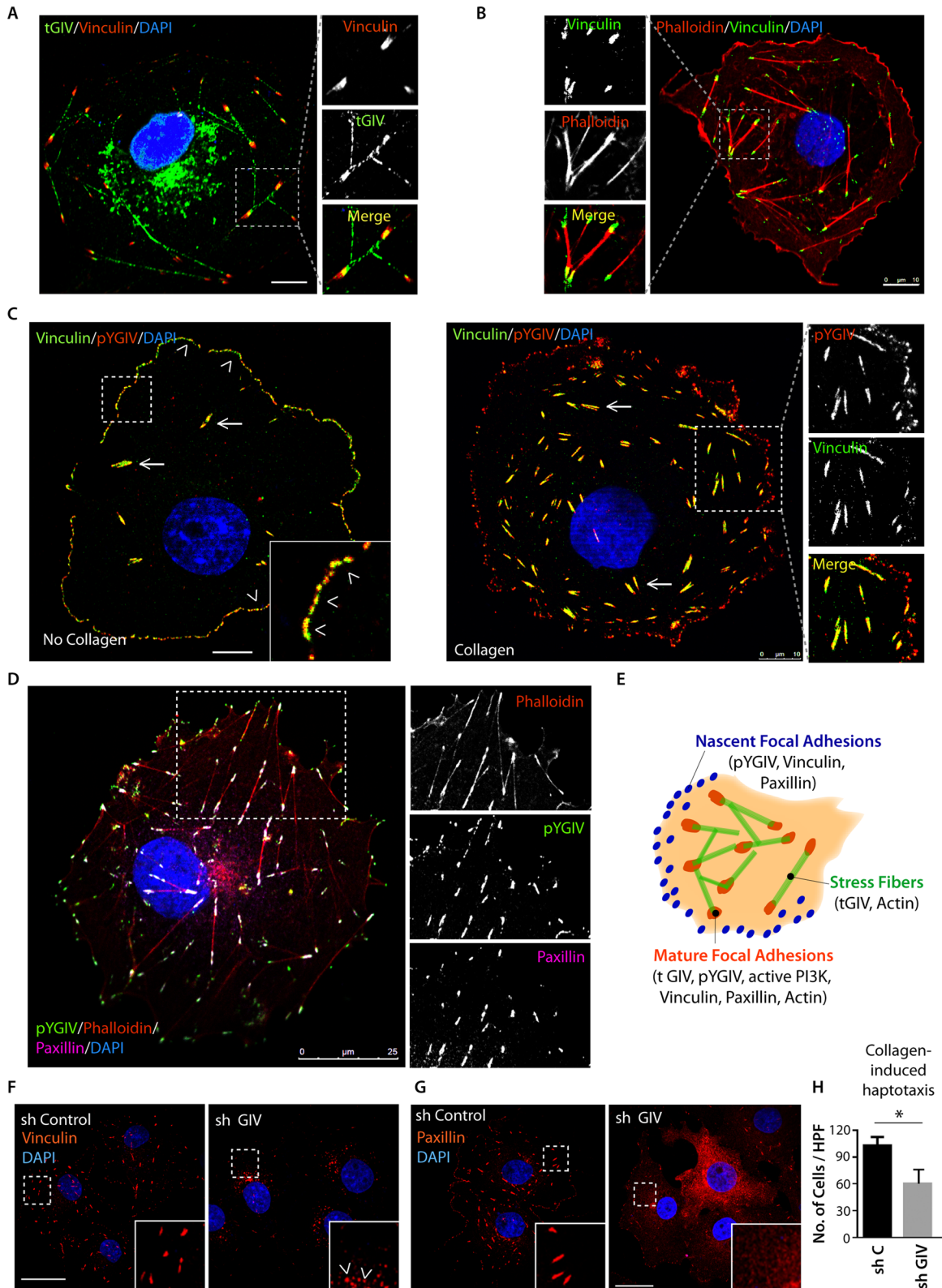
---

**FIGURE 1:** GIV localizes to FAs and is essential for the integrity of these structures. (A, B) Cos7 cells grown on collagen-coated coverslips were fixed and costained with GIV (green), vinculin (red), and DAPI (nuclei; blue; A) or with vinculin (green), phalloidin–Texas red (F-actin, red), and DAPI (nuclei; blue; B) and analyzed by confocal microscopy. Representative images. Bar, 10 μm. (C) Cos7 cells grown on either noncoated (left) or collagen-coated (right) glass coverslips, fixed, and costained with phospho-Tyr-1764-GIV (pYGIV; red), vinculin (green), and DAPI (nuclei; blue) and analyzed by confocal microscopy. Arrowheads indicated focal complexes; arrows indicate mature FAs. Representative images. Bar, 10 μm. (D) Cos7 cells were fixed and costained with phospho-Tyr-1764-GIV (pYGIV; green), phalloidin–Texas red (F-actin; red), paxillin (far red; pseudocolored purple), and DAPI (nuclei; blue) and analyzed by

specifically the localization of GIV at the PM without the noise contributed by the larger cytosolic pool, we carried out immunofluorescence studies on cells fixed using a low-temperature methanol-fixation treatment that leads to improved accessibility of the intracellular antigens and reduces cytosolic background (Schnell *et al.*, 2012). GIV localized to the Golgi, the nucleus, and actin stress fibers (Figure 1A), all previously reported by us and others (Enomoto *et al.*, 2005; Ghosh *et al.*, 2008). A pool of actin-bound GIV colocalized with vinculin, indicating that GIV localizes also on PM patches where actin caps associate with FAs (Figure 1B); this pattern is specific, because it was lost in GIV-depleted cells (Supplemental Figure S1A). When we immunostained for the tyrosine-phosphorylated pool of "active" GIV (pYGIV), as determined by a diagnostic-grade antibody previously validated and confirmed to specifically detect phospho-Tyr-1764-GIV (see *Materials and Methods*), we found it to be almost exclusively colocalized with vinculin in FAs: in the absence of collagen, pYGIV and vinculin colocalized predominantly in the peripherally located "environment-probing" focal complexes (Figure 1C, left), whereas in the presence of collagen, they colocalized primarily within mature FAs (Figure 1C, right). Localization of GIV at FAs was further confirmed using paxillin, another marker of FAs (Figure 1D and Supplemental Figure S1B). Finally, tyrosine-phosphorylated GIV localized to FAs in cells stimulated exclusively with collagen in the absence of serum (Supplemental Figure S1C), suggesting that integrin signaling is sufficient for both tyrosine phosphorylation and localization of GIV at FAs. These results indicate that a pool of total GIV and the majority of "active" pYGIV localize discretely to nascent and mature FAs (Figure 1E).

To determine the role of GIV at FAs, we analyzed GIV-depleted Cos7 cells (~85% depletion efficacy by short hairpin RNA [shRNA]; Supplemental Figure S1D) and found that, compared with controls, these cells had fewer FA structures (by ~80%, as determined by quantification of structures that immunostained for vinculin and paxillin [Figure 1, F and G] using the particle analyzer feature of ImageJ; Horzum *et al.*, 2015) and impaired collagen-induced motility (~40% reduction, as determined using Transwell haptotactic cell motility assays [Figure 1H and Supplemental S1E]). We conclude that GIV is an essential functional component within the FAs.

## GIV is a substrate of focal adhesion kinase
Because tyrosine-phosphorylated GIV is primarily restricted to FAs (Figure 1), we asked whether GIV is a substrate of the non-RTK focal adhesion kinase (FAK), a key component of the signal transduction pathways triggered by integrins whose activity is restricted to the FAs (Sulzmaier *et al.*, 2014). In vitro kinase assays on the histidine (His)-tagged C-terminus of GIV (GIV-CT) showed that such is indeed the case; GIV was phosphorylated at two critical sites, Tyr (Y)-1764 and -1798, by recombinant FAK, and no phosphorylation was observed using a mutant in which both tyrosines were replaced with Phe (YF; Figure 2A). Because the commercially obtained FAK used in these assays was purified from insect cells to >95% purity, we conclude that FAK phosphorylates GIV; it targets the two key tyro-

sines on GIV that were previously shown to directly bind Src-homology 2 domains of p85α (PI3K) and activate the p110 (PI3K) catalytic subunit (Lin *et al.*, 2011). FAK also phosphorylated GIV in cells because expression of the wild type but not the kinase-dead mutant FAK(K454R) in Cos7 cells triggered tyrosine phosphorylation of GIV (Figure 2B) and pharmacologic inhibition of FAK abolished tyrosine phosphorylation of GIV (Figure 2C). Immunofluorescence on Cos7 cells undergoing adhesion on collagen-coated surface showed that by 30 min, active FAK, as determined by phosphorylation of Y397 (Chen *et al.*, 1996), and active pYGIV colocalized extensively within nascent FAs at the cell periphery (Figure 2D). By 4 h, extensive colocalization was maintained but shifted to mature FAs (Figure 2D). Whereas ~50% of the cells showed pYGIV labeling of nascent FAs at the cell periphery without paxillin in those structures, the reverse (i.e., paxillin-labeled structures devoid of pYGIV) was never encountered (Supplemental Figure S1F). Thus the localization of active pYGIV to FAs coincided temporospatially with activated FAK and preceded the localization of paxillin to FAs.

Next we asked whether GIV and FAK interact in cells by performing proximity ligation assays (PLAs) to detect in situ active GIV-FAK complexes in Cos7 cells. PLA signals were detected between endogenous active GIV and FAK (Figure 2E and Supplemental Figure 2SA), indicating that they interact (i.e., the maximum distance between the two is ≤30–40 nm; Soderberg *et al.*, 2006). Taken together, these findings indicate that FAK binds and phosphorylates GIV and that such phosphoevents occur during the early stages of cell–extracellular matrix (ECM) adhesion within FAs, before paxillin is enriched at those locations. These observations are in keeping with the previously reported temporal and spatial dynamics of FAK activity during cell adhesion (Serrels and Frame, 2012). Because GIV is also a substrate of multiple RTKs and the non-RTK Src (Lin *et al.*, 2011) and those TKs also phosphorylate substrates within FAs, how much of the observed active pool of pYGIV at the FAs is a direct contribution of FAK remains to be determined.

## Tyrosine phosphorylation of GIV is required for enhancement of PI3K-Akt signals, integrity of FAs, cell adhesion, and haptotaxis
To analyze the role of tyrosine phosphorylation of GIV in signaling at the FAs, we rescued Cos7 cells that were depleted of endogenous GIV by stably expressing FLAG-tagged wild-type (WT) or various GIV mutants (YF, nonphosphorylatable; FA, GEF deficient; YF/FA, combination of both; Supplemental Figure S2, B and C). First we asked whether FAK enhances PI3K/Akt signaling via its substrate GIV. We found that the Akt signaling response that was triggered by collagen was blunted in cells expressing the nonphosphorylatable GIV-YF mutant compared with those expressing GIV-WT (Figure 2F). Compared to Cos7 cells expressing GIV-WT, GIV-YF cells also showed fewer FAs (~75% reduction; Figure 2, G and H), as determined by immunofluorescence for vinculin and paxillin, impaired cell–ECM adhesion (~45% reduction; Figure 2I), and reduced collagen-induced motility (~40% reduction; Figure 2J and Supplemental

confocal microscopy. Representative images are shown. Bar, 25 μm. (E) Schematic summarizing the findings in A–D. (F, G) Control (sh Control) or GIV-depleted (sh GIV) Cos7 cells were fixed and stained for vinculin (red, F) or paxillin (red, G) and DAPI (nuclei; blue) and analyzed by confocal microscopy. In GIV-depleted cells we found that vinculin was present on vesicular structures (arrowheads). Representative images are shown. Bar, 25 μm. Depletion of GIV was confirmed by immunoblotting (Supplemental Figure S1D). (H) Cos7 cells in F and G were analyzed for collagen-induced haptotactic cell motility using Transwell assays. Bar graphs show quantification of the number of migrated cells/high-power fields (HPF). Error bars represent mean ± SD; *n* = 3; *p < 0.05.
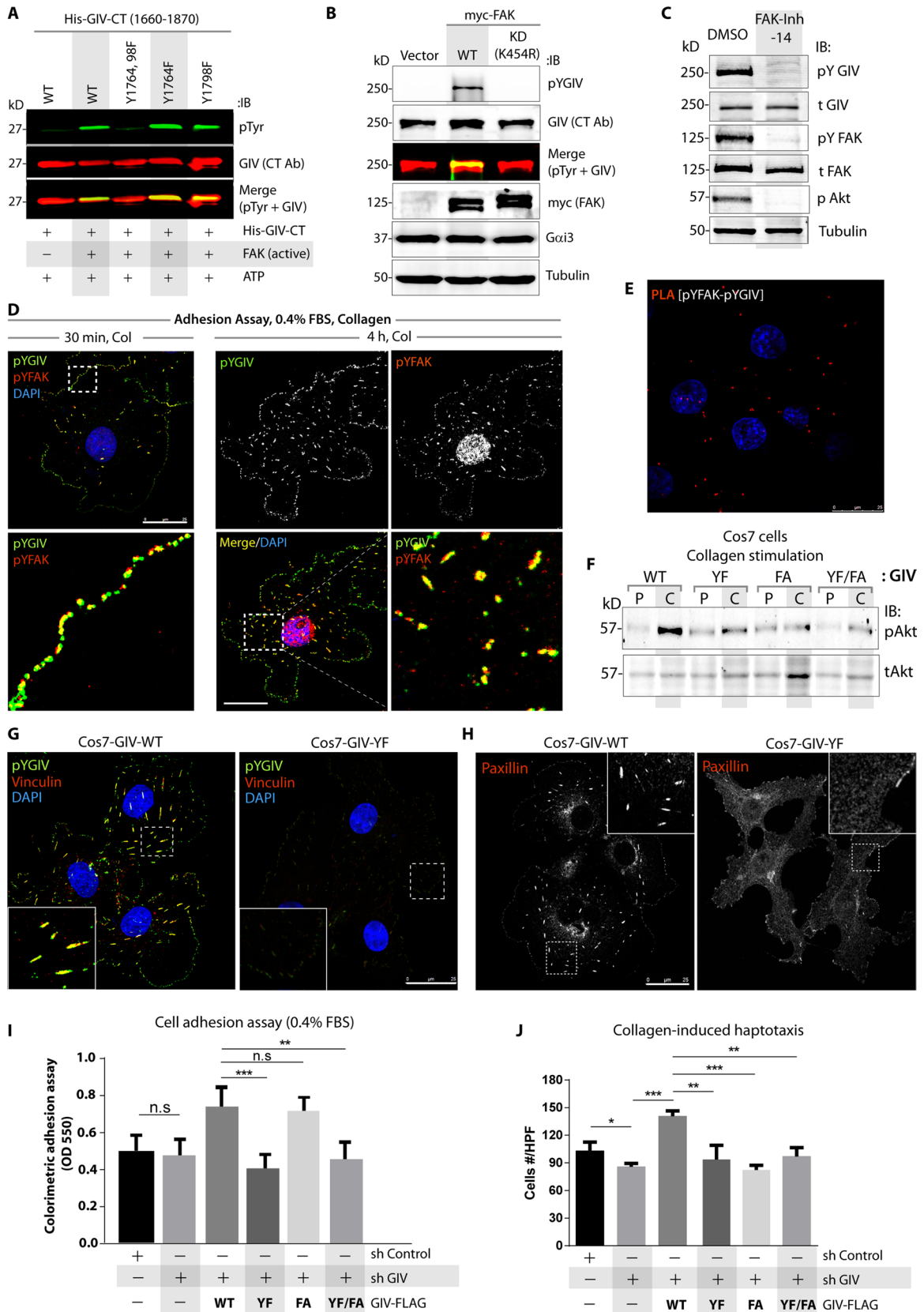
FIGURE 2: Phosphorylation of GIV by FAK is required for cell–ECM adhesion and collagen-induced haptotaxis. (A) In vitro kinase assays were carried out with recombinant FAK and equal aliquots of either WT or mutant His-GIV-CT (aa 1660–1870) proteins. Phosphorylated GIV was detected by immunoblotting using anti–phospho-Tyr antibody (top; green). His-GIV-CT proteins were visualized using GIV-CT antibody (middle; red). Yellow pixels in the merged panel represent tyrosine-phosphorylated GIV-CT. (B) Cos7 cells expressing control vector, wild-type FAK (myc-FAK-WT), or a

Figure S2D). These findings indicate that tyrosine phosphorylation of GIV is an essential step for the maximal activation of PI3K-Akt signals by FAK and for the functional integrity of FAs. Because phosphosites generated by FAK at tyrosines 1764 and 1798 on GIV can directly bind and activate PI3K (Lin et al., 2011), we conclude that GIV, a bona fide PI3K/Akt-enhancer (Lin et al., 2011), is a key substrate of FAK that enhances PI3K-Akt signals in response to ECM.

## Activation of Gαi by GIV enhances FAK activity and collagen-induced haptotaxis

Because GIV modulates signaling pathways by activating G proteins (Garcia-Marcos et al., 2015), next we asked how activation of Gi by GIV-GEF affects the integrity of FAs. We found that loss of FAs in GIV-depleted Cos7 cells was rescued by GIV-WT but not the GEF-deficient F1685A mutant of GIV (GIV-FA; Figure 3A and Supplemental Figure S3A); the latter cannot bind or activate Gαi (Garcia-Marcos et al., 2009). The cells expressing GIV-FA adhered as efficiently as those expressing GIV-WT in low serum (Figure 2I) but were disadvantaged in the presence of 10% serum (Figure 3B) and showed reduced haptotactic motility toward collagen (Figure 2J and Supplemental Figure S2D). As for the mechanism for such impaired haptotaxis, we found that activation of Akt was reduced in cells expressing GIV-FA (Figure 2F). This is in keeping with the fact that GIV's GEF function enhances PI3K/Akt signals via "free" Gβγ-intermediates (Garcia-Marcos et al., 2009) and, together with GIV's phosphotyrosines, maximally enhances Akt signaling in an "AND gate" mode (Lin et al., 2011), that is, both GEF and phosphotyrosines are required for maximal signaling. In addition, in cells expressing GIV-FA (Figure 3C) or depleted of GIV (Figure 3D), collagen-stimulated FAK activity, as determined by phosphorylation at Tyr-397 was also suppressed. Consistent with reduced activation of FAK, phosphorylation of its substrate, GIV at Tyr-1764 was similarly impaired (Figure 3A and Supplemental Figure S3A). Thus the GEF motif via which GIV activates Gαi is essential to maintain FA integrity, FAK and PI3K/Akt signaling, and collagen-induced chemotaxis.

The role of Gαi activation by GIV-GEF was further analyzed by expressing either wild-type (Gαi3-WT) or a dominant-negative W258F mutant of Gαi3, henceforth referred to as Gαi3-WF, in Cos7 cells; the latter cannot bind or be activated by GIV but localizes and interacts with Gβγ, GPCRs, and Gαi regulators similarly to Gαi3-WT (Garcia-Marcos et al., 2010). Compared to cells expressing Gαi3-WT, those expressing Gαi3-WF exhibited similar defects as observed in cells expressing GIV-FA; the number of FAs was reduced (by ~43%), as determined by staining for vinculin (Figure 3E and Supplemental Figure S3B) and FAK activation (Figure 3F and Supplemental Figure S3C), and phosphorylation of GIV (Supplemental Figure S3D) at the FAs were impaired. These results obtained using well-characterized and specific GIV (FA) and Gαi3 (WF) mutants that selectively block GIV's ability to bind and activate the G protein demonstrate that activation of Gi by GIV is key for maximal enhancement of FAK activity for the functional integrity of FAs during chemotaxis toward collagen.

Our findings are in keeping with previous studies that showed not only that G proteins localize to FAs (Hansen et al., 1994; Buhl et al., 1995; Ueda et al., 1997) and are active at that location (Gong et al., 2010), but also that Gαi activation by GPCRs affects FAK activity (Thennes and Mehta, 2012). We conclude that noncanonical Gi activation by the nonreceptor GEF GIV also affects the integrity of FAs, in part via enhancement of FAK activity.

## GIV colocalizes with and binds ligand-activated β1 integrins

Next we asked whether active GIV colocalizes with integrins and specifically examined β1 integrins, a major subunit of collagen I–binding integrins (Jokinen et al., 2004). Immunofluorescence studies confirmed that both total (Figure 4A) and active pYGIV (Figure 4B) colocalized with integrin clusters, as well as with bundles of β1 integrin, within 10 min after acute stimulation with collagen and continued to show more prominent colocalization at 30 min and 2 h (unpublished data).

Because several adaptors serve as mechanotransducers by directly binding to β-integrin cytoplasmic tails (Legate and Fassler, 2009) and GIV couples G proteins to a variety of receptors (Garcia-Marcos et al., 2015; Midde et al., 2015), next we asked whether GIV and Gαi interact with integrins. We found that both GIV and Gαi3 coimmunoprecipitate with β1 integrin exclusively after stimulation

kinase-dead mutant FAK (myc-FAK-KD) were analyzed by immunoblotting for phosphorylation of endogenous GIV using anti–phospho-Tyr-1764-GIV (pYGIV) antibody. Expression of FAK (myc), Gαi3, and tubulin was analyzed by immunoblotting. (C) Cos7 cells were grown on culture dishes coated with poly-D-lysine, treated with FAK inhibitor 14 (FAK-Inh-14) or vehicle (dimethyl sulfoxide [DMSO]) for 24 h, and then seeded on collagen-coated dishes for 1 h before lysis and analyzed for total (t) and phosphoproteins (p) by immunoblotting (IB). (D) Cos7 cells were acutely stimulated with collagen before fixation (see Materials and Methods) and stained with phospho–Tyr-1764-GIV (pYGIV; green), phospho–Tyr-397-FAK (pYFAK; red), and DAPI (nuclei; blue) and analyzed by confocal microscopy. Bar, 25 μm. (E) Cos7 cells were analyzed for interaction between active pYGIV and active pYFAK by in situ PLA using rabbit anti-pYGIV and mouse anti-pYFAK antibodies. Red dots indicate sites of interaction. Incubation with secondary antibodies alone or with paxillin antibody showed no signal (negative controls; Supplemental Figure S2A). Bar, 25 μm. (F) GIV-depleted Cos7 cells stably expressing FLAG-tagged WT or mutant GIV constructs were grown on culture dishes coated with poly-D-Lysine (P) and then seeded on collagen-coated (C) dishes for 1 h before lysis and analyzed for phospho (p-) and total (t-) Akt by immunoblotting (IB). Compared to GIV-WT cells, percentage phosphorylation of Akt was suppressed by 65% in GIV-YF cells, 82% in GIV-FA cells, and 73% in GIV-YF/FA cells (p < 0.001), as determined by band densitometry using LiCOR Odyssey. (G, H) GIV-depleted (sh GIV) Cos7 cells stably expressing GIV-WT or GIV-YF mutant were fixed and stained for phospho–Tyr-1764-GIV (pYGIV; green), vinculin (red), and DAPI (nuclei; blue; G) or for paxillin (red, shown in grayscale; H) and analyzed by confocal microscopy. Bar, 25 μm. (I) Colorimetric adhesion assays were carried out using control (sh Control), GIV-depleted (sh GIV), or GIV-depleted cells stably expressing various GIV constructs in media with low serum. Error bars represent mean ± SD; n = 3; **p < 0.01; ***p < 0.001; n.s, not significant. See also Supplemental Figure S2, B and C, for immunoblots showing the levels of GIV expression and other FA proteins in these cell lines. (J) Cells in I were analyzed for collagen-induced haptotactic cell motility using Transwell assays. Images of representative fields are displayed in Supplemental Figure S2D. Bar graphs show quantification of the number of cells that migrated averaged from ~ 20 high-power field-of-view images per experiment. Error bars represent mean ± SD; n = 3; *p < 0.05, **p < 0.01, ***p < 0.001.
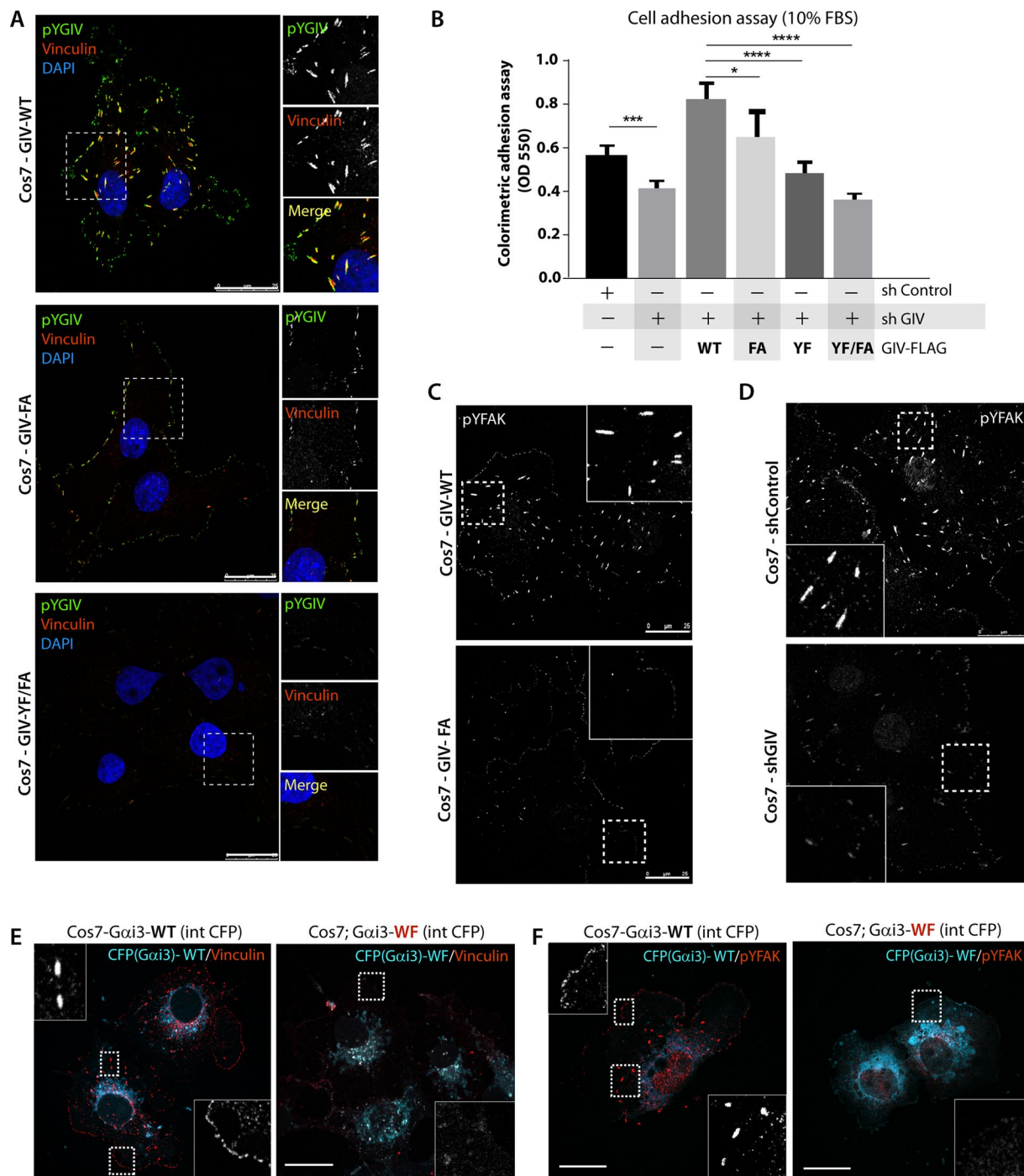
**FIGURE 3:** Activation of Gαi by GIV's GEF motif enhances FAK activity, the integrity of FAs, and cell–ECM adhesion.
(A) GIV-depleted Cos7 cells stably expressing GIV-WT, GIV-FA, or GIV-YF/FA were fixed and stained for phospho–Tyr-1764-GIV (pYGIV; green), vinculin (red), and DAPI (nuclei; blue) and analyzed by confocal microscopy. Bar, 25 μm.
(B) Colorimetric cell adhesion assay was carried out using control (sh Control), GIV-depleted (sh GIV) Cos7 cells, or those stably expressing GIV-WT or various mutants in the presence of 10% FBS. Error bars represent mean ± SD; $n = 3$; **$p < 0.01$, ***$p < 0.001$, ****$p < 0.0001$. (C) GIV-depleted Cos7 cells stably expressing GIV-WT or GIV-FA were fixed and stained for phospho–Tyr-397-FAK (pYFAK; shown in grayscale) and analyzed by confocal microscopy. Boxed areas are magnified and displayed as insets. Bar, 25 μm. (D) Control (sh Control) or GIV-depleted (sh GIV) Cos7 cells were fixed and stained for phospho–Tyr-397-FAK (pYFAK; shown in grayscale) as in C. Bar, 25 μm. (E) Cos7 cells transfected with internally tagged Gαi3-WT-CFP (cyan; left) or Gαi3-WF-CFP (cyan; right) were fixed and stained for vinculin (red) and analyzed by confocal microscopy. The red channel (vinculin) in the boxed areas is magnified and displayed in grayscale as inset. Individual channels are shown in Supplemental Figure S3B. Bar, 25 μm. (F) Cos7 cells in E were stained for pYFAK (red) and analyzed by confocal microscopy. Expression of Gαi3-WF reduced the intensity of pYFAK at FA structures by ~72%. The red channels (pYFAK) in the boxed areas are magnified and displayed in grayscale as inset. Individual channels are shown in Supplemental Figure S3C. Bar, 25 μm.
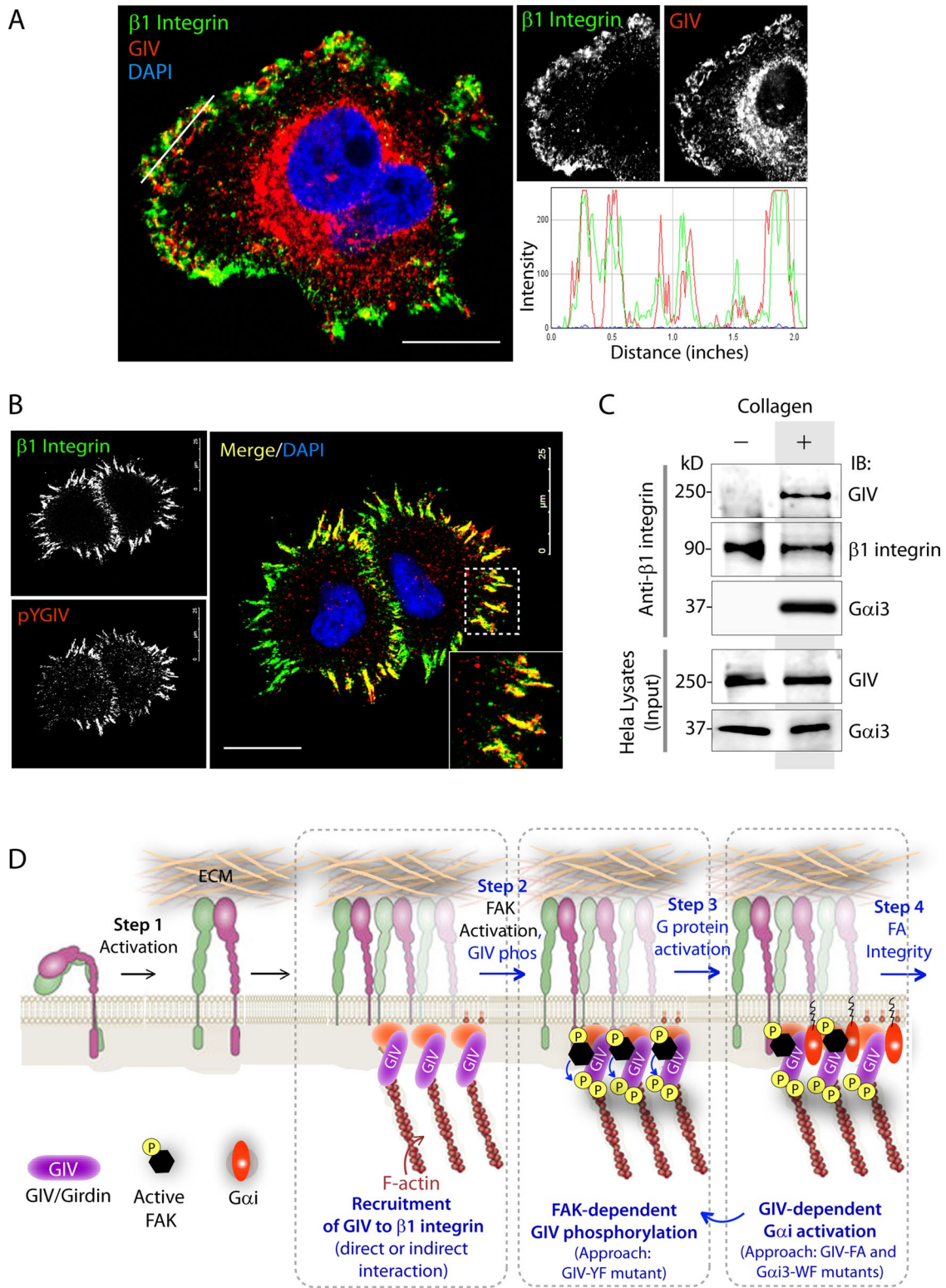
FIGURE 4: GIV colocalizes with bundles of β1 integrins and couples G proteins to β1 integrins. (A, B) HeLa cells grown on a poly-ᴅ-lysine–coated surface were resuspended, plated on collagen-coated surface for ~10 min, fixed, stained for β1 integrin (green), DAPI (nuclei; blue), and either GIV (red; A) or pYGIV (red; B) and analyzed by confocal microscopy. A line scan plot of relative fluorescence intensities of β1 integrin and GIV in A was analyzed using the RGB profiler plug-in from Image J. Bar, 25 µm. (C) HeLa cells grown on poly-ᴅ-lysine were stimulated (+) or not (−) with collagen and lysed, and the lysates were subjected to immunoprecipitation using anti–β1 integrin antibody. Immune complexes were analyzed for GIV, β1 integrin, and Gα3 by immunoblotting. (D) Schematic illustration summarizing how GIV-GEF modulates tyrosine-based and G protein signaling in the vicinity of ligand-activated β1 integrins.

with collagen (Figure 4C), indicating that GIV and G protein interact exclusively with ligand-stimulated β1 integrins.

Taken together, we propose the following working model (Figure 4D): GIV is recruited to ECM-activated β1 integrins, followed by phosphorylation of GIV by FAK. Such phosphorylation is triggered early during cell–ECM adhesion, a step in which GIV's GEF function is dispensable, whereas both GIV's phosphotyrosines and its GEF function are required during collagen-induced cell motility. When cell adhesion assays were carried out in the presence of 10% fetal bovine serum (FBS; as source of multiple growth factors), the importance of GIV's GEF function during cell–ECM adhesion was observed, indicating that activation of Gαi by GIV may potentiate FA functions in a growth factor–dependent manner. Thus the GEF-dependent enhancement of PI3K/Akt signaling we observe is likely to serve as a feedforward loop to enhance FAK activity, substrate (including GIV) phosphorylation, and cell adhesion/motility *specifically* in the presence of growth factors. The fact that the defects in cell adhesion/haptotaxis we observe in cells expressing a GEF-deficient GIV mutant (FA) and those that express a nonphosphorylatable GIV mutant (YF) are not additive in cells in which both are combined (GIV-YF/FA; Figures 2, I and J, and 3B and Supplemental Figure S2D) favors the model that GIV's GEF and phosphotyrosines work in a synergistic positive feedback loop.

## GIV maintains FA integrity in multiple cancer cells, and its activation is enhanced during metastatic progression

Because both GIV and FAK facilitate cancer progression (Ghosh et al., 2011; Sulzmaier et al., 2014), next we examined the distribution and function of GIV in multiple cancer cells. Tyrosine-phosphorylated GIV specifically localized to FAs across all cancer cell lines examined (Figure 5A and Supplemental Figure S4A). Depletion of GIV (by shRNA, ~75-85% efficacy; Supplemental Figure S4, B–D) resulted in a decrease of FAs, as determined by a shift of vinculin (Figure 5A) and paxillin (Supplemental Figure S4A) from FAs to the cytosol, reduced FAK activity (Figure 5B), and impaired ECM-induced cell motility (Figure 5C and Supplemental Figure S4E), indicating that GIV is an essential functional component of FAs in multiple cancer cells. To determine how phosphorylation of GIV and its localization at FAs changes during cancer invasion/metastasis, we used a well-characterized metastatic H2030 lung adenocarcinoma cell line and its corresponding highly metastatic subclone 3 (BrM3) that were selected in mice and display ~10-fold enhanced ability to metastasize to the bones and brain (Nguyen et al., 2009). Tyrosine-phosphorylated GIV showed a heterogeneous staining pattern (intensity and distribution). Despite heterogeneity, tyrosine-phosphorylated GIV colocalized with vinculin-positive FAs exclusively in the BrM3 clone (Figure 5, D–F). These findings indicate that metastatic progression is associated with increased association of active pYGIV with FAs.

In conclusion, we have shown that GIV is both an enhancer and a substrate of FAK and a multimodular linker between multiple components at FAs—for example, bundles of ECM-activated β1 integrins, the actin cytoskeleton, PI3-kinase/Akt, trimeric G protein, Gαi, and FAK. On the basis of our findings here that FAK and GIV-GEF cross-potentiate each other, we propose that mechanochemical signal integration via the FAK-GIV axis is essential for the functional integrity of FAs and enhanced ECM-induced motility. Aberrant activation of this FAK-GIV axis during cancer metastasis may fuel cancer progression.

## MATERIALS AND METHODS
### Reagents and antibodies
Unless otherwise indicated, all reagents were of analytical grade and obtained from Sigma-Aldrich (St. Louis, MO). Cell culture media were purchased from Invitrogen (Carlsbad, CA). Recombinant FAK protein was purchased from SignalChem (Richmond, Canada). FAK inhibitor 14 was purchased from Santa Cruz Biotechnology (Dallas, TX). All restriction endonucleases and *Escherichia coli* strain DH5α were purchased from New England Biolabs (Ipswich, MA). *E. coli* strain BL21 (DE3) and phalloidin–Texas red were purchased from Invitrogen. 4′,6-Diamidino-2-phenylindole (DAPI) was purchased from Molecular Probes (Invitrogen). Genejuice transfection reagent was obtained from Novagen (EMD Millipore; San Diego, CA) and TransIT-LT1 from Mirus Bio LLC (Madison, WI). Rat-tail collagen I was obtained from BD Biosciences and poly-D-lysine from Sigma-Aldrich. Puromycin was purchased from Life Technologies (Carlsbad, CA) and neomycin analogue G418 from Cellgro (Manassas, VA). Paraformaldehyde (PFA) 16% was purchased from Electron Microscopy Sciences.

Mouse monoclonal antibodies against Akt and β-tubulin and rabbit polyclonal antibodies against the last 18 amino acids (aa) of the C-terminus of GIV (GIV-CT, T-13), total FAK, β1 integrin (for immunoblotting and immunoprecipitation only), Gαi3 (M-14), and GFP were obtained from Santa Cruz Biotechnology. Rabbit antibody against phospho–Akt-Ser-473 was obtained from Cell Signaling (Beverly, MA). Mouse anti-vinculin, FLAG (M2), and polyhistidine were obtained from Sigma-Aldrich and anti–phospho-Tyr, phospho–FAK-Tyr397, and paxillin from BD Transduction Laboratories (San Jose, CA). Mouse β1 integrin antibody for immunofluorescence studies was obtained from Abcam (Cambridge, MA). Rabbit anti–GIV coiled-coil (GIV cc) was obtained from Millipore (San Diego, CA). The anti–phospho-GIV-Tyr-1764 rabbit monoclonal antibody (SP-158) of diagnostic grade was generated collaboratively with Ventana (a branch of Roche) and Spring Biosciences (Pleasanton, CA). Prior studies using this antibody confirmed that it specifically detects GIV phosphorylated at Y1764 but not the dephosphorylated protein (Lopez-Sanchez et al., 2014). Goat anti-rabbit and goat anti-mouse Alexa Fluor 680 or IRDye 800 F(ab′)2 used for Odyssey infrared imaging were from Li-Cor Biosciences (Lincoln, NE). Secondary goat anti-rabbit or mouse (488), goat anti-rabbit or mouse (594), and goat anti-mouse (635) Alexa-conjugated antibodies used for immunofluorescence were from Invitrogen (Life Technologies).

### Plasmid constructs and protein expression
Cloning of GIV-CT (aa 1660–1870) into pET28b (His-GIV CT) was described previously (Garcia-Marcos et al., 2009). For mammalian expression, RNA interference–resistant (shRNA rest) GIV was cloned into p3XFLAG-CMVTM-14 plasmid (GIV-FLAG) as described previously (Garcia-Marcos et al., 2009). GIV-FLAG and His-GIV-CT phosphomutants (Y1764F, Y1798F, and Y1764/1798F) and GEF-deficient mutant (F1685A) were generated by site-directed mutagenesis using a QuikChange kit (Stratagene) and specific primers (sequence available upon request) as per the manufacturer's protocols (Garcia-Marcos et al., 2009; Lin et al., 2011). Internally tagged Gαi3-WT-CFP was a generous gift from Moritz Bünemann, Philipps-Universität Marburg, Marburg, Germany (Bünemann et al., 2003). Gαi3-WF-CFP mutant (Garcia-Marcos et al., 2010) was generated by site-directed mutagenesis using QuikChange per the manufacturer's protocol. Primer sequences are available upon request. shRNA 3–untranslated region for GIV (GIV shRNA: CCGGGCTTTCATTACC AGCTCTGAACTCGAGTTCAGAGCTGGTAATGAAAGCTTTTTTG) was cloned into pLKO.1 (TRCN0000130452) or control vector TRC1.5-pLKO.1-puro. pKH3-FAK-WT and pKH3-FAK-K454R were generous gifts from Jun-Lin Guan (University of Michigan, Ann Arbor, MI).

His-GIV-CT fusion construct was expressed in *E. coli* strain BL21 (DE3) and purified as described previously (Ghosh et al., 2008,
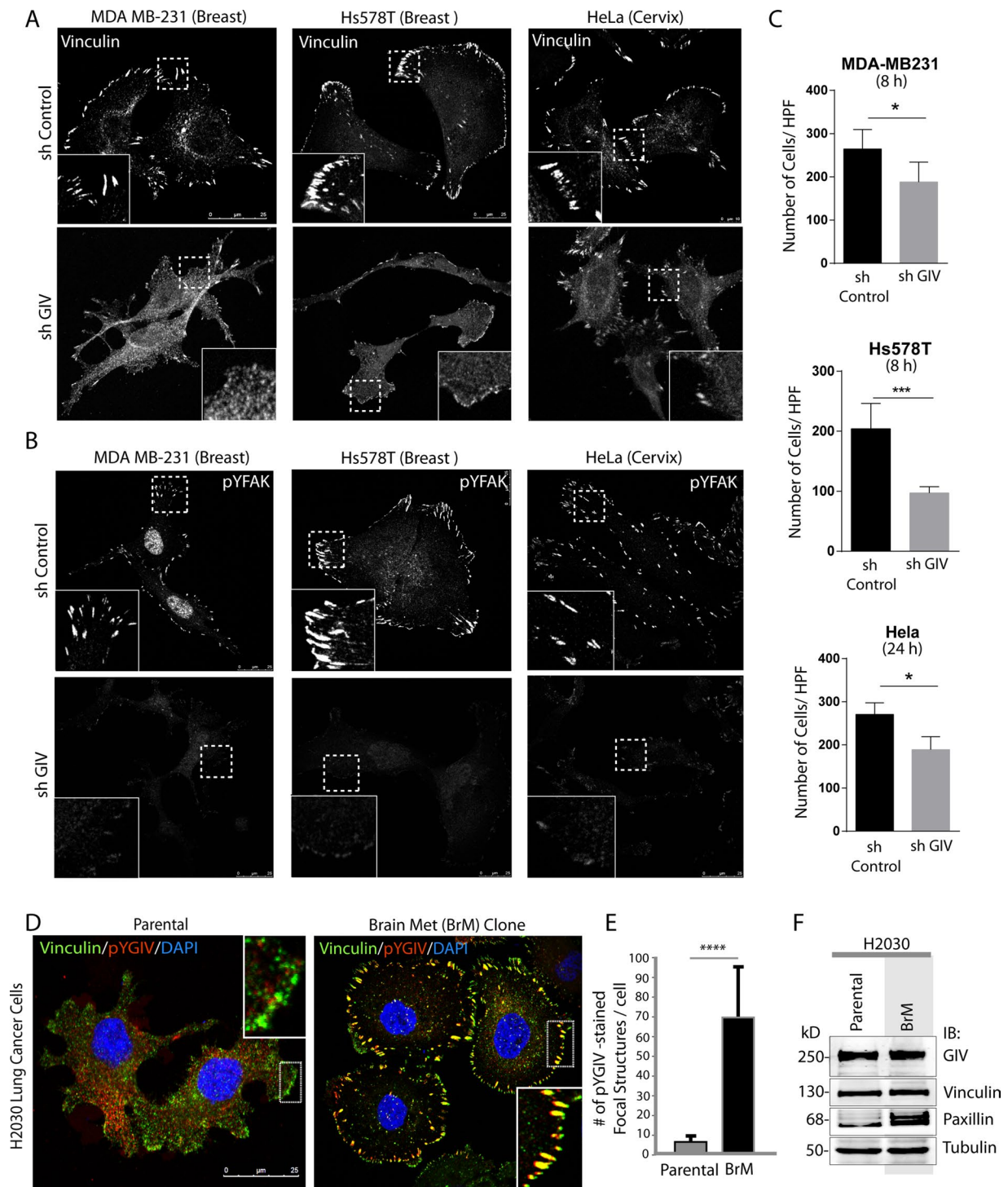
**FIGURE 5:** GIV is essential for the integrity of FAs and ECM-induced chemotaxis in metastatic cancer cells. Control (sh Control) or GIV-depleted (sh GIV) MDA MB-231 (left), Hs578T (middle), and HeLa (right) cells were fixed and stained for vinculin (A) or pYFAK (B) and analyzed by confocal microscopy. Bar, 25 μm. Depletion of GIV was confirmed by immunoblotting (Supplemental Figure S4, B–D). (C) Cell lines in A were analyzed for collagen-induced haptotactic cell motility using Transwell assays as in Figure 1H. Bar graphs show quantification of the number of migrating cells per high-power field (HPF). Data are presented as mean ± SEM; $n = 3$. Representative fields of the Transwell membrane are shown in Supplemental Figure S4E. *$p < 0.05$, ***$p < 0.001$. (D) Parental H2030 (left) and its corresponding metastatic BrM subclone (right) were fixed and stained for phospho–Y1764-GIV (pYGIV; red), vinculin (green), and DAPI (nuclei; blue) and analyzed by confocal microscopy. Representative fields are shown. Bar, 25 μm. (E) Bar graphs show quantification of the number of pYGIV-stained, vinculin-positive FA structures per cell in D (y-axis) determined using ImageJ. Error bars represent mean ± SD. ****$p < 0.0001$. (F) Immunoblotting of whole-cell lysates of cells in D showed similar levels of GIV, vinculin, and tubulin.

2010; Garcia-Marcos et al., 2009). Briefly, bacterial cultures were induced overnight at 25°C with 1 mM isopropyl β-D-1-thiogalactopyranoside (IPTG). Pelleted bacteria from 1 l of culture were resuspended in 10 ml of His lysis buffer (50 mM $NaH_2PO_4$, pH 7.4, 300 mM NaCl, 10 mM imidazole, 1% [vol:vol] Triton X-100, 2× protease inhibitor cocktail [Complete EDTA-free, Roche Diagnostics, Pleasanton, CA]). After sonication (3 × 30 s), lysates were centrifuged at 12,000 × g at 4°C for 20 min. Solubilized proteins were affinity purified on HisPur Cobalt Resin (Pierce, Rockford, IL). Proteins were eluted, dialyzed overnight against PBS, and stored at –80°C.

## Whole-cell immunofluorescence
Cells were fixed at room temperature with 3% PFA in PBS for 25 min, treated with 0.1 M glycine for 10 min, and subsequently permeabilized for 20 min (0.2% Triton X-100 in PBS) and blocked in PBS containing 1% bovine serum albumin (BSA) and 0.1% Triton X-100 as described previously (Lopez-Sanchez et al., 2014). Primary and secondary antibodies where incubated for 1 h at room temperature in blocking buffer. In the case of total GIV (tGIV) immunofluorescence, cells were fixed using 100% methanol at –20 °C for 10 min, followed by blocking buffer. ProLong (Life Technologies) was used as mounting medium.

Dilutions of antibodies used were as follows: GIVcc, 1:250; phospho–Tyr-1764-GIV, 1:300; vinculin, 1:400; paxillin, 1:200; integrin-β1, 1:400; phalloidin, 1:1000; phospho-FAK, 1:100; DAPI, 1:2000; and secondary goat anti-rabbit (488), goat anti-mouse (594), and goat-anti-mouse (635) Alexa-conjugated antibodies, 1:500.

Images were acquired at room temperature with a Leica TCS SPE-II with DMI4000 microscope equipped with a Leica Hamamatsu 9100-02 camera and the LAS AF SPE software (Leica) using a 63× oil-immersion objective using 488-, 561-, 635-, and 405-nm laser lines for excitation. The settings were optimized and the final images scanned with line averaging of three scans. Quantification of focal adhesions was carried out using the particle analyzer application on ImageJ (National Institutes of Health, Bethesda, MD) exactly as outlined previously (Horzum et al., 2015). All images were processed using ImageJ software and assembled for presentation using Photoshop and Illustrator software (Adobe, San Jose, CA). Images shown are representative of 90–95% cells that were evaluated across three independent experiments.

## In vitro kinase assay
These assays were performed using purified His-GIV CT proteins (~5 μg) and commercially obtained FAK kinase (SignalChem, Richmond, Canada) as previously described (Lin et al., 2011). Briefly, reactions were started by addition of 1000 μM ATP and carried out at 25°C for 60 min in 30 μl of kinase buffer (60 mM HEPES, pH 7.5, 5 mM $MgCl_2$, 5 mM $MnCl_2$, 3 μM $Na_3OV_4$). Reactions were stopped by addition of Laemmli sample buffer and boiling. Phosphorylated His-GIV-CT proteins were detected by immunoblotting.

## In cellulo kinase assay
These assays were carried out exactly as outlined previously (Lin et al., 2011). Briefly, Cos7 cells coexpressing GIV-FLAG with either WT or kinase-dead mutant FAK kinase were pretreated with 0.1 μM $Na_3OV_4$ for 1 h before lysis. Lysates were separated by SDS–PAGE and analyzed by immunoblotting with anti-pYGIV antibody.

## Generation of stable cell lines
shRNA control and shRNA GIV Cos7, HeLa, MDA-MB-231, and Hs578T stable cell lines using MissionRNAi technology (Sigma-Aldrich) were generated by lentiviral transduction followed by selec-

tion with puromycin (2.5 μg/ml, except for Hs578T cells, for which it was 1 μg/ml). Depletion of endogenous GIV was confirmed by immunoblotting with GIV-CT rabbit antibody.

Lentiviral packaging was performed in HEK293T cells by cotransfecting the shRNA constructs with psPAX2 and pMD2G plasmids (4:3:1 ratio, respectively), using Mirus LT1. The medium was changed after 24 h, and virus-containing medium was collected after 36–48 h and centrifuged and filtered through a 0.45-μm filter. psPAX2 and pMD2G plasmids were a generous gift from Christopher K. Glass (University of California, San Diego, La Jolla, CA).

shRNA GIV Cos7 stable cell lines expressing p3xFLAG-CMV-14-GIV (GIV-3xFLAG) WT, FA, 2YF, and FA/2YF constructs were selected as previously described (Garcia-Marcos et al., 2009; Lopez-Sanchez et al., 2013) with the neomycin analogue G418 at 800 μg/ml. Expression of various GIV constructs were confirmed to be similar to levels of endogenous GIV in shRNA control cells by immunoblotting with GIV-CT and FLAG antibodies.

## Proximity ligation assay
In situ interaction of endogenous active GIV (identified by anti-pTyr-1764) with active FAK (identified by anti-pTyr-397) was detected using the proximity ligation assay kit Duolink (Olink Biosciences, Uppsala, Sweden). Fixation, permeabilization, and blocking were done as described for whole-cell immunofluorescence. The PLA assay was performed according to the manufacturer's recommendations. As negative control, cells incubated with only secondary antibodies were used.

## Cell culture, transfection, lysis, and quantitative immunoblotting
Unless mentioned otherwise, cell lines used in this work were cultured according to American Type Culture Collection (ATCC) guidelines or guidelines previously published for each line. H2030 parental and its brain metastatic (BrM3) counterpart were a generous gift from Joan Massagué (Memorial Sloan Kettering Cancer Center, New York, NY; Nguyen et al., 2009; Valiente et al., 2014). Cos7, HeLa, and Hs578T cells were obtained from ATCC.

Transfection, lysis, and immunoblotting were carried out exactly as described before (Ghosh et al., 2008, 2010). Cells were transfected using Genejuice or Mirus LT1 following the manufacturers' protocols. For assays involving serum starvation, serum concentration was reduced to 0% FBS overnight. Whole-cell lysates were prepared after washing cells with cold PBS before resuspending and boiling them in sample buffer. Lysates used as a source of proteins in pull-down assays were prepared by resuspending cells in lysis buffer (20 mM HEPES, pH 7.2, 5 mM Mg acetate, 125 mM K acetate, 0.4% Triton X-100, and 1 mM dithiothreitol supplemented with sodium orthovanadate [500 μM], phosphatase [Sigma-Aldrich], and protease [Roche] inhibitor cocktails), after which they were passed through a 28-gauge needle at 4°C and cleared (10,000 × g for 10 min) before use in subsequent experiments. For immunoblotting, protein samples were separated by SDS–PAGE and transferred to polyvinylidene fluoride membranes (Millipore). Membranes were blocked with PBS supplemented with 5% nonfat milk (or with 5% BSA when probing for phosphorylated proteins) before incubation with primary antibodies. Infrared imaging with two-color detection and quantification were performed using a Li-Cor Odyssey imaging system. Dilution of primary antibodies used were as follows: anti–GIV-CT, 1:500; anti–phospho-Tyr-1764-GIV, 1:500; anti–phospho-Ser-473-Akt, 1:250; anti-Akt, 1:500; anti-Gαi3, 1:333; anti-vinculin, 1:500; anti-paxillin, 1:500; anti-β tubulin, 1:1000; anti-myc, 1:250; anti-FLAG, 1:250; anti-β1 integrin, 1:250; and anti–phospho-Tyr397-FAK,

1:250. All Odyssey images were processed using ImageJ software and assembled for presentation using Photoshop and Illustrator software.

## Transwell migration assay

Cell migration was assessed using Costar Transwell inserts with 8-µm pores in 24-well plates. The bottom sides of the membrane filters were coated with 50 µg/ml type I collagen at 4°C overnight, washed twice in PBS, and then blocked with 0.5% BSA for 2 h at 37°C. Cells were detached using trypsin/EDTA and resuspended in DMEM supplemented with 0.4% FBS. A total of $5 \times 10^4$ cells was loaded in the upper well in a volume of 300 µl, and the lower well was filled with 750 µl of DMEM with 0.4% FBS. The plates were incubated at 37°C for the indicated periods of time before removing the remaining cell suspension. The migration insert was placed in a clean well containing 4% PFA for 1 h at room temperature, stained with Giemsa for 1 h, and washed three times in PBS. Cells on the upper side of the filters were removed with cotton-tipped swabs, and the number of migrated cells on the bottom side of the filter was counted in five randomly chosen fields at 200× magnification and averaged. All experiments were performed in triplicate, and each experiment was repeated at least three times.

Colorimetric cell adhesion assay 96-well microtiter plates were coated with collagen, rinsed with PBS, and then blocked with 0.5% BSA for 1 h at 37°C. Cells were harvested with trypsin/EDTA, seeded in the wells at $2 \times 10^4$ cells/well in 50 µl of DMEM with 10 or 0.4% FBS, and allowed to adhere for 1 h at 37°C. Nonadherent cells were removed by gentle washing twice with PBS, and attached cells were fixed in 4% PFA for 15 min and then stained with 2.3% crystal violet (Sigma-Aldrich) for 10 min. Cells were extensively washed, air dried, and then lysed with 100 µl of 2% SDS. The absorbance of the wells was measured at 600 nm in a microplate reader. All experiments were performed in triplicate, and each experiment was repeated at least three times.

## Immunoprecipitation

HeLa cell lysates (~2 mg of protein) treated or not with collagen were incubated for 3 h at 4°C with 2 µg of anti–β1 integrin monoclonal antibody or preimmune control mouse immunoglobulin G. Protein G–Sepharose beads (GE Healthcare, Wauwatosa, WI) were added and incubated at 4°C for an additional 60 min. Beads were washed, and bound immune complexes were eluted by boiling in nonreducing Laemmli sample buffer.

## Data analysis and other methods

All experiments were repeated at least three times, and results were presented either as one representative experiment or as average ± SD. Statistical significance was assessed with the Student's $t$ test. $*p < 0.05$, $**p < 0.01$, $***p < 0.001$, $****p < 0.0001$.

## REFERENCES

Buhl AM, Johnson NL, Dhanasekaran N, Johnson GL (1995). G alpha 12 and G alpha 13 stimulate Rho-dependent stress fiber formation and focal adhesion assembly. J Biol Chem 270, 24631–24634.

Bünemann M, Frank M, Lohse MJ (2003). Gi protein activation in intact cells involves subunit rearrangement rather than dissociation. Proc Natl Acad Sci USA 100, 16077–16082.

Chen HC, Appeddu PA, Isoda H, Guan JL (1996). Phosphorylation of tyrosine 397 in focal adhesion kinase is required for binding phosphatidylinositol 3-kinase. J Biol Chem 271, 26329–26334.

Enomoto A, Murakami H, Asai N, Morone N, Watanabe T, Kawai K, Murakumo Y, Usukura J, Kaibuchi K, Takahashi M (2005). Akt/PKB regulates actin organization and cell motility via Girdin/APE. Dev Cell 9, 389–402.

Garcia-Marcos M, Ghosh P, Ear J, Farquhar MG (2010). A structural determinant that renders G alpha(i) sensitive to activation by GIV/girdin is required to promote cell migration. J Biol Chem 285, 12765–12777.

Garcia-Marcos M, Ghosh P, Farquhar MG (2009). GIV is a nonreceptor GEF for G alpha i with a unique motif that regulates Akt signaling. Proc Natl Acad Sci USA 106, 3178–3183.

Garcia-Marcos M, Ghosh P, Farquhar MG (2015). GIV/Girdin transmits signals from multiple receptors by triggering trimeric G protein activation. J Biol Chem 290, 6697–6704.

Ghosh P (2015). Extra views: G protein coupled growth factor receptor tyrosine kinase: no longer an oxymoron. Cell Cycle 14, 2561–2565.

Ghosh P, Beas AO, Bornheimer SJ, Garcia-Marcos M, Forry EP, Johannson C, Ear J, Jung BH, Cabrera B, Carethers JM, Farquhar MG (2010). A G{alpha}i-GIV molecular complex binds epidermal growth factor receptor and determines whether cells migrate or proliferate. Mol Biol Cell 21, 2338–2354.

Ghosh P, Garcia-Marcos M, Bornheimer SJ, Farquhar MG (2008). Activation of Galphai3 triggers cell migration via regulation of GIV. J Cell Biol 182, 381–393.

Ghosh P, Garcia-Marcos M, Farquhar MG (2011). GIV/Girdin is a rheostat that fine-tunes growth factor signals during tumor progression. Cell Adh Migr 5, 237–248.

Gong H, Shen B, Flevaris P, Chow C, Lam SC, Voyno-Yasenetskaya TA, Kozasa T, Du X (2010). G protein subunit Galpha13 binds to integrin alphaIIbbeta3 and mediates integrin "outside-in" signaling. Science 327, 340–343.

Hansen CA, Schroering AG, Carey DJ, Robishaw JD (1994). Localization of a heterotrimeric G protein gamma subunit to focal adhesions and associated stress fibers. J Cell Biol 126, 811–819.

Hartung A, Ordelheide AM, Staiger H, Melzer M, Haring HU, Lammers R (2013). The Akt substrate Girdin is a regulator of insulin signaling in myoblast cells. Biochim Biophys Acta 1833, 2803–2811.

Horzum U, Ozdil B, Pesen-Okvur D (2015). Differentiation of normal and cancer cell adhesion on custom designed protein nanopatterns. Nano Lett 15, 5393–5403.

Jokinen J, Dadu E, Nykvist P, Kapyla J, White DJ, Ivaska J, Vehvilainen P, Reunanen H, Larjava H, Hakkinen L, Heino J (2004). Integrin-mediated cell adhesion to type I collagen fibrils. J Biol Chem 279, 31956–31963.

Legate KR, Fassler R (2009). Mechanisms that regulate adaptor binding to beta-integrin cytoplasmic tails. J Cell Sci 122, 187–198.

Lin C, Ear J, Midde K, Lopez-Sanchez I, Aznar N, Garcia-Marcos M, Kufareva I, Abagyan R, Ghosh P (2014). Structural basis for activation of trimeric Gi proteins by multiple growth factor receptors via GIV/Girdin. Mol Biol Cell 25, 3654–3671.

Lin C, Ear J, Pavlova Y, Mittal Y, Kufareva I, Ghassemian M, Abagyan R, Garcia-Marcos M, Ghosh P (2011). Tyrosine phosphorylation of the Galpha-interacting protein GIV promotes activation of phosphoinositide 3-kinase during cell migration. Sci Signal 4, ra64.

Lopez-Sanchez I, Dunkel Y, Roh YS, Mittal Y, De Minicis S, Muranyi A, Singh S, Shanmugam K, Aroonsakool N, Murray F, et al. (2014). GIV/Girdin is a central hub for profibrogenic signalling networks during liver fibrosis. Nat Commun 5, 4451.

Lopez-Sanchez I, Garcia-Marcos M, Mittal Y, Aznar N, Farquhar MG, Ghosh P (2013). Protein kinase C-theta (PKCtheta) phosphorylates and inhibits the guanine exchange factor, GIV/Girdin. Proc Natl Acad Sci USA 110, 5510–5515.

Midde KK, Aznar N, Laederich MB, Ma GS, Kunkel MT, Newton AC, Ghosh P (2015). Multimodular biosensors reveal a novel platform for activation

of G proteins by growth factor receptors. Proc Natl Acad Sci USA 112, E937–E946.

Nguyen DX, Chiang AC, Zhang XH, Kim JY, Kris MG, Ladanyi M, Gerald WL, Massague J (2009). WNT/TCF signaling through LEF1 and HOXB9 mediates lung adenocarcinoma metastasis. Cell 138, 51–62.

Schnell U, Dijk F, Sjollema KA, Giepmans BN (2012). Immunolabeling artifacts and the need for live-cell imaging. Nat Methods 9, 152–158.

Serrels B, Frame MC (2012). FAK and talin: who is taking whom to the integrin engagement party? J Cell Biol 196, 185–187.

Soderberg O, Gullberg M, Jarvius M, Ridderstrale K, Leuchowius KJ, Jarvius J, Wester K, Hydbring P, Bahram F, Larsson LG, Landegren U (2006). Direct observation of individual endogenous protein complexes in situ by proximity ligation. Nat Methods 3, 995–1000.

Sulzmaier FJ, Jean C, Schlaepfer DD (2014). FAK in cancer: mechanistic findings and clinical applications. Nat Rev Cancer 14, 598–610.

Thennes T, Mehta D (2012). Heterotrimeric G proteins, focal adhesion kinase, and endothelial barrier function. Microvasc Res 83, 31–44.

Ueda H, Saga S, Shinohara H, Morishita R, Kato K, Asano T (1997). Association of the gamma12 subunit of G proteins with actin filaments. J Cell Sci 110, 1503–1511.

Valiente M, Obenauf AC, Jin X, Chen Q, Zhang XH, Lee DJ, Chaft JE, Kris MG, Huse JT, Brogi E, Massague J (2014). Serpins promote cancer cell survival and vascular co-option in brain metastasis. Cell 156, 1002–1016.

Wang H, Misaki T, Taupin V, Eguchi A, Ghosh P, Farquhar MG (2015). GIV/girdin links vascular endothelial growth factor signaling to Akt survival signaling in podocytes independent of nephrin. J Am Soc Nephrol 26, 314–327.